HHS Public Access

Author manuscript

Clin Cancer Res. Author manuscript; available in PMC 2020 March 15.

Published in final edited form as:

Clin Cancer Res. 2019 September 15; 25(18): 5503–5512. doi:10.1158/1078-0432.CCR-19-0104.

High-plex predictive marker discovery for melanoma immunotherapy treated patients using Digital Spatial Profiling

Maria I. Toki[1], **Christopher R. Merritt**[2], **Pok Fai Wong**[1], **James Smithy**[3], **Harriet Kluger**[4], **Konstantinos Syrigos**[4,5], **Giang T. Ong**[2], **Sarah E. Warren**[2], **Joseph M. Beechem**[2], **David L. Rimm**[1,4]

[1]Department of Pathology, Yale School of Medicine, New Haven, CT

[2]NanoString Technologies®, Seattle, WA

[3]Brigham and Women's Hospital Department of Medicine, Boston, MA

[4]Department of Internal Medicine, Yale School of Medicine, New Haven, CT

[5]3rd Department of Medicine, University of Athens, School of Medicine, Sotiria General Hospital, Athens, Greece.

Abstract

Background—Protein expression in formalin-fixed, paraffin-embedded (FFPE) tissue is routinely measured by immunohistochemistry (IHC) or quantitative fluorescence (QIF) on a handful of markers on a single section. Digital Spatial Profiling (DSP) allows spatially-informed simultaneous assessment of multiple biomarkers. Here we demonstrate the DSP technology using a 44-plex antibody cocktail to find protein expression that could potentially be used to predict response to immune therapy in melanoma.

Methods—The NanoString GeoMx™ DSP technology is compared with automated QIF (AQUA) for immune marker compartment-specific measurement and prognostic value in Non-Small Cell Lung Cancer(NSCLC). Then we use this tool to search for novel predictive markers in a cohort of 60 immunotherapy (ITx) treated melanoma patients on a TMA using a 44-plex immune marker panel measured in three compartments (macrophage, leukocyte and melanocyte) generating 132 quantitative variables.

Results—The spatially informed variable assessment by DSP validates by both regression and variable prognostication compared to QIF for stromal CD3, CD4, CD8, CD20 and PD-L1 in NSCLC. From the 132 variables, 11 and 15 immune markers were associated with prolonged progression free survival (PFS) and overall survival (OS). Notably, we find PD-L1 expression in CD68 positive cells (macrophages) and not in tumor cells, was a predictive marker for PFS, OS and response.

*Corresponding Author: David L. Rimm M.D.-Ph.D., Professor of Pathology Director, Yale Pathology Tissue Services, Dept. of Pathology, BML 116, Yale University School of Medicine, 310 Cedar St. PO Box 208023, New Haven, CT 06520-8023, Phone: 203-737-4204, FAX: 203-737-5089, david.rimm@yale.edu.

Potential Conflict of Interest: Dr. Rimm declares that in the last two years he has served as a consultant to Astra Zeneca, Agendia, Amgen, Bethyl Labs, Biocept, BMS, Cell Signaling Technology, ClearSight, Daiichi Sankyo, InVicro/Konica-Minolta, Navigate Biopharma, Merck, OptraScan, Perkin Elmer, and Ultivue. Dr. Merritt, Mr. Ong, Dr. Warren, and Dr. Beechem declare that they are employees and shareholders of NanoString Technologies.

Conclusion—DSP technology shows high concordance with QIF and validates based on both regression and outcome assessment. Using the high-plex capacity we found a series of expression patterns associated with outcome including that the expression of PD-L1 in macrophages is associated with response.

Keywords

NanoString; multiplex; melanoma; PD-L1; biomarker

INTRODUCTION

Immune checkpoint inhibitors (ICIs) have dramatically changed the treatment landscape of many tumor types and altered therapeutic paradigms after the discovery of the immune checkpoint receptor programmed death 1 (PD-1) and its activator ligand, programmed death ligand-1 (PD-L1). PD-1 is expressed on the surface of Tumor Infiltrating Lymphocytes (TILs) and engages PD-L1 on tumor cells and/or other immune cells, and this interaction has been shown to be a major immune-inhibitory mechanism in the tumor microenvironment (TME) [1, 2]. Even though regulation of PD-1/PD-L1 pathway is a well characterized immune evasion mechanism, it has been reported that PD-1 checkpoint blockade mediates immune resistance in less than 40% of malignancies [3–5]. Tumor PD-L1 expression has been shown to predict response to immunotherapy [6, 7], although even with selection, the majority of patients fail to respond to PD-1 inhibitors [8]. Furthermore, patients with low tumor PD-L1 expression have also been reported to have durable responses [9].

Immunohistochemistry (IHC) analysis of formalin-fixed, paraffin-embedded (FFPE) patient tissue is currently the only companion diagnostic test in clinical practice. Despite its widespread use, its sensitivity, specificity and reproducibility are suboptimal and it offers limited information about the complexity of TME. In the light of the toxicity and high cost of checkpoint inhibitors, there is a need for biomarkers that can more accurately select patients that will benefit from immunotherapy [7, 10–14]. In order to optimize patient stratification, some recent studies have focused on the assessment of multiple variables in order to create signatures or a scoring system that takes into account transcriptomic data, tumor mutational burden and/or TILs infiltration [15–17]. Furthermore, assays that measure the expression of multiple immune markers can be used to reveal underlying mechanisms of tumor immune evasion in the TME, which may lead to the development of novel therapeutic strategies.

Quantitative immunofluorescence (QIF) is a technique that enables spatially resolved multiplexed target measurement on a single formalin fixed paraffin embedded (FFPE) tissue slide but is limited by the number of fluorescence channels that can be utilized[18]. NanoString DSP is a novel platform that offers nondestructive simultaneous high-plex quantitative measurement of biomarkers on a single FFPE tissue section within specific regions of interest. Regions of interest can be manually or molecularly defined. These features make the DSP platform well suited to discovery of single biomarkers or multiplexed signature development where target localization is important. In this study, we validate the quantitative localized measurement capability of NanoString DSP using automated QIF

(AQUA) as a criterion standard for immune marker compartment-specific measurement. Additionally, we assess their agreement on the prognostic value of CD3, a known prognostic biomarker of survival in Non-Small Cell Lung Cancer (NSCLC)[19]. Then we explore the predictive value of a 44-plex panel of immune markers in a cohort of immunotherapy treated melanoma patients. We identify PD-L1 expression in the macrophages, but not in the tumor, as the parameter that is most predictive of outcome. Furthermore, we identify an additional 26 potential biomarkers, illustrating the potential of the platform for discovery of novel biology and biomarkers.

MATERIALS AND METHODS

Tissue Microarray (TMA) and patient cohorts

Tissue specimens were prepared in a tissue microarray format as previously described [20]. Representative tumor areas were obtained from formalin-fixed, paraffin-embedded (FFPE) specimens and 0.6mm cores from each tumor block were arrayed in a recipient block. FFPE cell line pellets, tonsil and placenta were used as controls. YTMA 356 (Yale cohort A), is a Non-Small Cell Lung Cancer (NSCLC) array that consists of primary tumors resected between 2010–2014 from 43 patient cases that received Epidermal Growth Factor Receptor (EGFR) Tyrosine Kinase Inhibitors (TKIs) at some point after resection. It includes 36 EGFR mutant, 6 EGFR wild type and 1 of unknown mutation status patient tumors as well as 14 cell line cores (H820, H1648, H1993, H441, H1299, A431, A549, H2882, HCC193, HT29, PC9, MCF7, SKBR3, H1355). A previously described cohort [21], YTMA 79 (Yale cohort B), consists of 202 FFPE primary NSCLC tumors from patients seen at Pathology Department of Yale University between 1988 and 2003. YTMA 376 (Yale cohort C), consists of 60 FFPE melanoma patient tumors resected between 2011 and 2016 initially described by Wong et al[22]. The data cut-off date was September 1, 2017 and the median follow up time was 20.1 months. All patients in this cohort received ICIs after specimen collection. All cohorts consist of retrospectively serially collected tumors without stratification or matching and clinicopathological information from patients was collected from clinical records and pathology reports. Detailed characteristics of each cohort are presented in Supplemental Tables S1–S3.

All tissue was used in accordance with US Common Rule after approval from the Yale Human Investigation Committee protocol #9505008219 with an assurance filed with and approved by the U.S. Department of Health and Human Services. Approval includes informed written consent or in some cases waiver of consent.

Quantitative Immunofluorescence (QIF)

Quantitative measurement of PD-L1 and TILs markers was performed using AQUA™ method (Navigate Biopharma, Carlsbad, CA), quantifying fluorescent signal within subcellular compartments, as described previously [23]. A tumor mask was created by binarizing the cytokeratin signal and creating an epithelial/melanocyte compartment. When this compartment size was less than 2% of the area of the TMA spot, the spot was excluded. Stroma was defined as the remaining area with positive DAPI staining. Quantitative immunofluorescence (QIF) score was calculated by dividing the target pixel intensity by the

area of the compartment. QIF scores were normalized to the exposure time and bit depth at which the images were captured, allowing scores collected at different exposure times to be comparable.

Digital Spatial Profiling

The NanoString digital spatial profiling technology allows specially defined collection of oligonucleotides tags that are cleaved from specific validated antibodies. The regions of interest may be user defined (drawn on an image) or molecularly defined using a fluorescence image of the same slide prior to collection. Here, FFPE tissue slides were incubated with cocktails of up to 44 unique oligonucleotide-conjugated antibodies (Suppl Table 4). The compartments were identified with fluorescent imaging with antibodies targeting cytokeratin to detect NSCLC tumor compartment and S100 with HMB45 for melanocytes, CD68 for macrophages and CD45 for leukocyte detection. Target immune markers were measured by sequential compartment assignment of the macrophage, leukocyte and finally tumor compartment. The selected compartments were chosen for high-resolution multiplex profiling, and oligos from the selected region were released upon exposure to UV light. Photocleaved oligos were then collected via microcapillary tube inspiration using an early version of the DSP platform (NanoString, Seattle WA) robotic system and transferred into a microwell plate with a spatial resolution of approximately 10 μm. Photocleaved oligos from the spatially-resolved compartments in the microplate were then hybridized to 4-color, 6-spot optical barcodes in the nCounter® platform, enabling up to 800 distinctly labels counts in per compartment of the protein targets representing the antibodies to which the tags were originally conjugated. Digital counts from barcodes corresponding to protein probes were first normalized with internal spike-in controls (ERCCs) to account for system variation, and then normalized to the area of their compartment.

Multiplexed TILs and TILs activation Immunofluorescence Staining

The multiplexing TIL protocol has been published[24]. Briefly, tissue sections were subjected to the same deparaffinization, antigen retrieval, and blocking protocol mentioned above. Staining for pan-cytokeratin, CD4, CD8, and CD20 was performed using a sequential multiplexed immunofluorescence protocol with isotype-specific primary antibodies to detect epithelial tumor cells (cytokeratin: clone Z0622, Agilent, Santa Clara, CA), helper T cells (CD4 IgG, 1:100, clone SP35, Spring Bioscience, Pleasanton, CA), cytotoxic T cells (CD8 IgG1, 1:250, clone C8/144B, Agilent, Santa Clara, CA), and B lymphocytes (CD20 IgG2a, 1:150, clone L26, Agilent, Santa Clara, CA). Nuclei were highlighted using 4’,6-Diamidino-2-Phenylindole (DAPI). Secondary antibodies and fluorescent reagents used were goat anti-rabbit Alexa546 (Molecular Probes, Eugene, OR, USA), anti-rabbit Envision (K4009, Agilent, Santa Clara, CA) with biotynilated tyramide/Streptavidine-Alexa750 conjugate (Perkin-Elmer, Waltham, MA), anti-mouse IgG1 antibody (1:100, eBioscience, San Diego, CA) with fluorescein-tyramide (Perkin-Elmer, Waltham, MA), anti-mouse IgG2a antibody (1:200, Abcam, Cambridge, MA) with Cy5-tyramide (Perkin-Elmer, Waltham, MA). Residual horseradish peroxidase activity between incubations with secondary antibodies was eliminated by exposing the slides twice for seven minutes to a solution containing benzoic hydrazide (0.136 gr) and hydrogen peroxide (50 μl).

Staining for T-cell activation panel[25] included pan-cytokeratin, CD3, Ki67, and Granzyme B and was performed using a similar sequential multiplexed immunofluorescence protocol with isotype-specific primary antibodies to detect epithelial tumor cells (cytokeratin, clone Z0622, 1:100, Agilent, Santa Clara, CA), T lymphocytes (CD3 IgG, 1:100, clone SP7, Novus Biologicals, Littleton, CO), Ki67 (IgG1, 1:100, clone MIB-1, Agilent, Santa Clara, CA), and Granzyme B (IgG2a, 1:2000, clone 4E6, Abcam, Cambridge, MA). Fresh control slides from morphologically normal human tonsil were included in each staining batch as positive controls and to ensure reproducibility.

PD-L1 Immunofluorescence Staining

Tissue sections were subjected to the same deparaffinization, antigen retrieval, and blocking protocol mentioned above and incubated overnight with a cocktail of the primary target antibody, PD-L1 (9A11, Cell Signaling Technology, Danvers, MA) mouse monoclonal antibody, and a cytokeratin antibody, rabbit polyclonal antibody (Z0622, Agilent, Santa Clara, CA). Next, sections were incubated for 60 minutes at room temperature with Alexa 546-conjugated goat anti-rabbit secondary antibody (Molecular Probes, Eugene, OR) diluted 1:100 in mouse EnVision amplification reagent (K4001, Agilent, Santa Clara, CA). Cyanine 5 (Cy5) directly conjugated to tyramide (FP1117, Perkin-Elmer, Waltham, MA) at a 1:50 dilution for 10 minutes was used for target detection and ProLong gold mounting medium (Molecular Probes, Eugene, OR) containing DAPI was used to stain nuclei. Control slides were run for reproducibility alongside each experimental slide-staining run.

Statistical Analysis

Pearson's correlation coefficient (R) was used to assess the agreement between QIF scores and DSP counts from near serial sections of Yale Cohort A (YTMA 356). Overall survival (OS) and Progression Free Survival (PFS) curves were constructed using the Kaplan-Meier analysis with a follow up of 60 months and statistical significance was determined using the log-rank test. For the statistical analysis, the average NanoString counts from two available cores of each case was used. All p-values were based on two-sided tests and p-values <0.05 were considered statistically significant for median stratification. For markers stratified by any other cutpoint, the significance cut-off was set after Bonferroni correction for multiple comparisons. Specifically, for markers stratified by tertiles, a p-value<0.0167 was considered significant while for quartile stratification a difference would be considered statistically significant if the p-value<0.0083. Statistical analyses were performed using IBM SPSS Version 20 (IBM Corp., Armonk, NY), JMP Pro software (version 11.2.0, 2014, SAS Institute Inc, Cary, NC) and GraphPad Prism v6.0 for Windows (GraphPad Software, Inc, San Diego, CA). All tumor spots were visually evaluated and cases with staining artifacts or presence of less than 2% tumor compartment area were systematically excluded.

RESULTS

DSP standardization to QIF and validation

In order to validate the NanoString DSP platform, we used the AQUA method of QIF as a comparison standard in Yale cohort A that contains NSCLC patients treated with EGFR TKIs. The compartment assignment method of the two assays is similar, as both use positive

immunofluorescence signal to create compartments within a Region of Interest (ROI) in which multiple targets are measured. Briefly, imaging of fluorophore-conjugated cytokeratin-specific antibody is used to create a binary mask which directs UV light to only the tumor compartment within a field of view. DNA oligos are released from the oligo-conjugated antibodies via cleavage of the UV photocleavable linker, collected, hybridized to reporter probes, and counted as tumor markers on the NanoString nCounter System. The stoma compartment is collected by inverting the mask and collecting the remaining oligos within the compartment. Visually, the compartments created by both assays were found to be comparable (Suppl. Figure 1). Regression of counts and QIF scores for multiple immune markers in tumor and stroma regions showed a high concordance between the two assays. Specifically, for CD3 (R^2=0.68), CD4 (R^2=0.55), CD20 (R^2=0.74) and CD8 (R^2=0.54) there was a strong agreement when those markers were measured in the stroma compartment in near serial section TMAs (Figure 1A–D). Counting PD-L1 by NanoString DSP in tumor compartment had a higher degree of agreement to PD-L1 tumor QIF scores (R^2=0.53) compared to stroma measurements (R^2=0.13), which can be attributed to a higher heterogeneity of immune cells expressing PD-L1 across sections (Figure 1E–F) or the variance in compartment assignment between the two methods. As Yale cohort A is an EGFR TKI treated cohort of NSCLC patients, we also investigated whether any of the immune markers measured by NanoString DSP had a predictive role in response, PFS and OS, but none of them was found to be associated with favorable outcome (data not shown).

As a further step to validation, we used a second NSCLC cohort (Yale cohort B) to test whether stratification of patients by stromal CD3 counts measured by NanoString DSP technology reproduced the prognostic significance found by QIF. Stratification of patients by median QIF measured stromal CD3 counts in tumor (Figure 2A) showed a statistically significantly enrichment of OS in the CD3-high samples (p=0.0019 HR:0.41, 95% CI: 0.24–0.72). Similarly, high CD3 in stroma by QIF (Figure 2B) was associated with favorable prognosis (p=0.036 HR: 0.55, 95% CI: 0.32–0.96). Measurement of CD3 in the tumor by DSP (Figure 2C) had a similar prognostic value (p=0.034 HR: 0.54, 95% CI: 0.30–0.95) to QIF, but for stroma counts (Figure 2D) the statistical difference did not reach significance (p=0.26 HR: 0.73 95% CI: 0.42–1.27) perhaps due to lower resolution definition of stroma. This further demonstrates that there is a high concordance between the two assays when the measurements are performed in the same compartments on a field of view averaged basis, which was further validated by comparing prognostic significance.

Discovery of immunotherapy predictive markers for melanoma

To test the capacity of the DSP technology to discover multiple or novel immune related biomarkers associated with response and survival, we used a melanoma immunotherapy treated cohort of patients (Yale cohort C) and measured 44 markers simultaneously in three different compartments. Representative images of a TMA spot and the compartments are shown in Figure 3A–B. The three molecular compartments were defined by the detection of fluorescence-labeled primary antibodies targeting CD68 for macrophages (Figure 3C), CD45 for leukocytes (Figure 3D) and S100 plus HMB45 for melanocyte detection (Figure 3E). Target immune markers were measured by sequential compartment assignment of the macrophage, leukocyte and finally tumor compartment. The remaining DNA positive area

(the fourth compartment) was inadequate for further assessment (Figure 3F). As Nanostring DSP utilizes molecular definition of compartment assignment and not cell segmentation, measurement of marker co-expression on a per cell basis was not generated. Molecular definition of compartments is more similar to the AQUA method of quantitative fluorescence, and thus not subject to the reproducibility errors that are more common with software-based cell segmentation. However, a limitation of this approach is that is does not allow measurements on a “per cell” basis. Each patient case was represented by 2 non-adjacent TMA cores collected in separate runs from two independent TMA master blocks. As validation of the reproducibility of DSP, the agreement of target count measurement for all markers between the two cores from separate TMA blocks, on different days, was assessed. The reproducibility for CD8 and CD68 (R^2=0.49 and R^2=0.7, respectively) across the two cores in two independent experiments is shown in Suppl. Figure 2A–B. This level of reproducibility is comparable to that seen by QIF where the lower R^2 values are a function of tissue heterogeneity, not lack of analytic reproducibility.

Furthermore, as the collection of the DNA oligonucleotides for marker measurement was performed sequentially and the resolution for compartment separation was approximately 10 μm in this version of the instrumentation, we observed that the detection of a given target was affected by target abundance as well as order of compartment collection. In overlapping or close proximity compartments, measurement of a marker can appear to be associated with a non-expressing cell type. For example, since CD68+ compartments were collected first, followed by CD45+ compartments, we observed counts for CD8, a well characterized marker of cytotoxic T-cells, in both CD68+ and CD45+ compartments (Figure 3G). Interestingly, high CD8 counts in the CD68 compartment (Figure 4A–C), were found to be associated with prolonged OS (p=0.0119, HR: 0.33, 95% CI: 0.14–0.78) and PFS (p=0.0082, HR: 0.42, 95% CI: 0.22–0.83) as well as response to immunotherapy (p=0.014) while CD8 in the CD45+ compartment was not. Similarly, CD8 in the melanocyte compartment was predictive of favorable outcome. Rather than mis-assignment, these observations may be seen as a low-resolution molecular proximity assay. While proximity assays usually include enzymatic activation steps for the detection of proximity between two markers, here the 10um resolution of markers’ expression assignment to the neighboring compartment can serve as an indirect proximity indication.

Overall, by unadjusted univariable analysis, we found 11 markers associated with longer PFS (Table 1). As this was an exploratory study, we tested multiple cut points (median, tertiles, quartiles) for significance. In the tumor compartment, high CD8, CD3, TIM3, HLADR, IDO1 (tertiles) and CD11c were predictive for PFS; in macrophages, high CD8, beta-2-microglobulin (B2M), PD-L1 (tertiles), and TIM3 were predictive; and in lymphocytes, high B2M was predictive. Fifteen markers were found to have a statistically significant univariate association to longer overall survival (Table 2). In tumor, high CD8, B2M, CD20, IDO1 (tertiles) and HLADR were predictive; in macrophages, high CD8, CD4, B2M, PDL1 (tertiles), and CD3, but low PMS2 and MYC were predictive; and in lymphocytes, high B2M but low PMS2 and MSH2 (tertiles) were predictive. Low PD-1 expression in lymphocytes (1^{st},2^{nd} and 3^{rd} vs 4^{th} quartile) showed a trend toward prolonged PFS and OS (p=0.0084 and p=0.44 respectively) (Suppl. Figure S3B–C). Multivariate

analysis for PFS and OS (Table S5–S6) by each compartment showed that only PDL1 in macrophages remained statistically significant for OS.

Notably, PD-L1 expression in macrophages was associated with prolonged OS (p=0.0032, HR: 0.15, 95% CI: 0.065–0.35) and PFS (p=0.0072, HR: 0.36, 95% CI: 0.18–0.69), while PD-L1 expressed in lymphocytes and melanocytes did not have any statistically significant predictive value. PD-L1 expression in macrophages could also distinguish responders from non-responders to immunotherapy regardless of tumor PD-L1 expression (p=0.0011) (Figure 4D–I). PD-L1 expression in tumor was found to be modestly correlated to macrophage PD-L1, suggesting an adaptive upregulation mechanism to immune pressure (Suppl. Figure 3A). Further subgroup analysis of lymphocytes by PD-L1 expression revealed that high PD-L1 expression was associated with higher levels of B2M (p<0.0001), HLADR (p=0.0004), IDO1 (p<0.0001), TIM3 (p=0.0001) and B7H4 (p=0.0069), while high PD-1 expressing lymphocytes had significantly higher expression of BIM (p=0.0124), GZMB (p=0.0091) and BCL6 (0.01).

DISCUSSION

In this study, we benchmarked the novel digital spatial profiling technology against an established platform, and then used it to identify novel candidate predictors of response to immunotherapy. First, we used the AQUA method of QIF, a method thoroughly used and previously compared to Mass Spectrometry[26], for validation of the technology. We found that there is a high correlation between measurements by the two assays in a large number of patient cases with multiple markers (CD3, CD4, CD8, CD20 and PD-L1) measured in tumor and stroma compartments. Additionally, CD3 measurement by DSP reproduced the prognostic value similar to that seen using AQUA, as previously described[27].

In order to utilize the high-plex capacity of DSP to identify novel candidate biomarkers, we used a TMA consisting of a cohort of 60 pretreatment biopsies from melanoma patients treated with immunotherapy to determine the clinical significance of a panel of 44 immune related markers measured in three different compartments simultaneously (macrophages, lymphocytes and melanocytes). A total of 11 and 15 immune markers were found to be correlated to PFS and OS respectively, many of which have not been described before in this spatial context. For example, HLA-DR expression has been described on macrophages as a marker of activation and antigen presentation [28–30], cytotoxic T-lymphocytes (CTLs) and melanoma cells [31]. Here, HLA-DR expression in melanoma cells is associated with outcome in ICI treated patients, representing a potential new finding that needs further validation.

This study complements two recent reports which utilized DSP to investigate predictive biomarkers of survival in the adjuvant/neoadjuvant therapeutic setting for melanoma. In the first, DSP profiling was conducted on core needle biopsies from metastases-containing lymph nodes of patients with advanced melanoma [32] and the compartment profiled was defined by a geometric area of the tissue. PD-L1 was observed to be associated with relapse free survival following either adjuvant or neoadjuvant combination therapy with ipilimumab and nivolumab. In the second study, DSP was performed on tumor tissue taken either at baseline or on treatment with neoadjuvant nivolumab or the neoadjuvant combination of

nivolumab and ipilimumab, and CD45+ cells were profiled as a compartment [33]. Here, expression of a number of targets were associated with relapse free survival in either arm, including PD-1, B2M, MS4A1, CD8A, CD45RO, GZMB, CD3, CD19, KI-67, VISTA and CD4. This, these studies found in common a role for B2M, CD3, CD4, CD8A, PD-1 and PD-L1 in melanoma response to immunotherapy. This study further identified TIM3, MSH2, and MYC as potential biomarkers of response in the immune cell compartments, and 9 additional potential biomarkers in the tumor compartment.

In our study, CD3 and CD8 in the macrophage compartment was also found to be associated with prolonged survival. CD3+ and CD8+ cell infiltration has been previously reported to correlate with favorable outcome to immunotherapy treatment [34, 35]. Similarly, the role of macrophage and CD8+ cell interaction has been described[36], as macrophages mediate lymphocytic trapping and the blockade of Colony Stimulating Factor 1 Receptor (CSF1R) increases responsiveness to anti-PD-1 treatment. A recent study [37] on 104 primary stage II/III melanoma tumors showed that a low CTL/macrophage ratio correlated with shortened OS and that close distance to macrophages also indicated poor prognosis. In our study, CD3 and CD8 expression assigned to CD68 compartment was associated with better outcome in immunotherapy treated melanoma tumors. This highlights the importance of spatial information when measuring immune targets, as CD8 that was assigned to macrophage or tumor compartments due to proximity, were the ones carrying the predictive value of the marker, while no clinical significance was found for expression in CD45+ compartment, approximating CD8 cells at a greater distance to macrophage or tumor cells. Again, this finding needs to be validated in other cohorts, but it supports the concept that CD8 close to macrophages is more important than total CD8.

Arguably the most interesting finding in the study was the association of PD-L1 expression in macrophages with overall survival. Although there was a trend towards prolonged PFS and OS for tumor PD-L1 expression, it did not reach statistical significance (p=0.054 and p=0.072 respectively) (Figure 4G–I). While this could be an artifact of imperfect compartmentalization and a part of PD-L1 tumor expression could have been measured in the macrophage compartment, emerging evidence supports the predictive value of PD-L1 macrophage over tumor expression. Tumor PD-L1 expression is the most commonly used predictive marker for response to ICIs and represents the only currently approved companion diagnostic. It is predictive in both tumor cells (in lung cancer) and immune cells (in breast cancer, and probably gastric, cervical, bladder and head and neck squamous cell carcinoma[38–41]. While immunes cells are not specifically classified, they are considered to predominantly include lymphocytes and macrophages, along with smaller numbers of other immune effector cells (myeloid derived suppressor cells, natural killer cells and others). There is growing evidence though that PD-L1 expression by macrophages may be a key element driving response to PD-L1 antibody treatment. Previous studies have shown that targeting PD-1/PD-L1 axis can still be effective regardless of PD-L1 tumor expression [3, 42, 43] with 83% of NSCLC and 46% of all tumor types with IHC score 3 of tumor infiltrating immune cells responding to treatment [43]. A recent study [44] also showed that treatment of mouse and human macrophages with PD-L1 antibodies increased macrophage proliferation, survival and antitumor activity and that PD-L1 treatment exerted antitumor activity in mice lacking T cells, findings that are consistent with T-cell–independent,

macrophage-dependent antitumor activity. Two mechanistic studies in mouse models also support macrophages as the key effector cell in the PD-axis mechanism of inhibition. Lin and colleagues found that neither knockout nor overexpression of PD-L1 in tumor cells had an effect on PD-L1 blockade efficacy in mice with expression of PD-L1 in macrophages [45]. Similarly, Tang and colleagues found that PD-1 axis drug efficacy was not seen in myeloid PD-L1 −/− mice which was restored by transplantation of myeloid PD-L1 WT/WT cells [46]. Further studies are underway to determine the role of macrophage PD-L1 expression in anti-tumor immune response.

There are a number of limitations to this study. Firstly, both DSP and AQUA assays were done on TMAs that are not currently used in the clinical setting. For immune markers that often have a high level of heterogeneity, accurate representation of the tumor and the TME is essential. For our study, we used two non-adjacent TMA cores for each patient in order to minimize sampling errors, but realize this still represents a very small percentage of a standard tissue section. However, the use of TMAs allowed the assessment of 44 immune markers included in the DSP panel in a large number of patients in a pilot study setting. Another limitation of the study is that the melanoma cohort consisted of patients that received a variety of immunotherapies, including combination therapies, but were all analyzed in unison. Response to the different therapies may be driven by distinct biology which requires unique signatures to achieve greatest predictive power. Another limitation of this work is inherent in the DSP method. This method is limited to about 10μm resolution which means that some immune cells that infiltrate the tumors may be missed and mis-assigned to the tumor compartment. This issue may be addressed in the future as the DSP resolution is increased. Finally, only a single cohort of immunotherapy treated patients was available for this study, which precludes validation of the biomarkers in an independent cohort or the use of more stringent statistical analysis and biomarker stratification. Future studies with additional samples from multiple institutes, conducted on a validated platform such as QIF, will be required to evaluate these biomarkers and develop diagnostic signatures. Similarly, subclassification of macrophages and lymphocytes or other cells (NKT) for immune marker measurement by immune cell types will provide more information about their role in antitumor immunity. These studies are beyond the scope of this pilot work and we look forward to assessing more compartments in future efforts.

In conclusion, we validated NanoString DSP technology as a new method for high-plex measurement of immune markers in multiple compartments and used it to discover over 20 potentially predictive markers of response to immunotherapy in melanoma patients. Among them, the association of PD-L1 expression in macrophages with overall survival confirms mechanistic findings in mouse models in human tissue and gives a new insight in the clinical significance of macrophages in anti-tumor effect after PD-1/PD-L1 pathway blockade in melanoma patients. This study illustrates the potential to leverage high-plex profiling on DSP to characterize tumor biology, elucidate drug mechanisms of action and identify novel biomarkers associated with clinical response to therapy.

Supplementary Material

Refer to Web version on PubMed Central for supplementary material.

Acknowledgments

This work was supported by grants from the NIH including the Yale SPORE in Lung Cancer, P50-CA196530 and the Yale Cancer Center Support Grant P30-CA016359 and the SU2C Lung Cancer Dream Team Funding. The authors also acknowledge the expert assistance of Lori Charette and her staff in the Yale Tissue Microarray Facility division of Yale Pathology Tissue Services for construction of the tissue microarrays used in the study.

REFERENCES

1. Keir ME, Butte MJ, Freeman GJ, et al. PD-1 and its ligands in tolerance and immunity. Annu Rev Immunol 2008;26:677–704. [PubMed: 18173375]
2. Sharpe AH, Wherry EJ, Ahmed R, et al. The function of programmed cell death 1 and its ligands in regulating autoimmunity and infection. Nat Immunol 2007;8:239–245. [PubMed: 17304234]
3. Taube JM, Anders RA, Young GD, et al. Colocalization of inflammatory response with B7-h1 expression in human melanocytic lesions supports an adaptive resistance mechanism of immune escape. Sci Transl Med 2012;4:127ra137.
4. Zhang Y, Chen L. Classification of Advanced Human Cancers Based on Tumor Immunity in the MicroEnvironment (TIME) for Cancer Immunotherapy. JAMA Oncol 2016;2:1403–1404. [PubMed: 27490017]
5. Sznol M, Chen L. Antagonist antibodies to PD-1 and B7-H1 (PD-L1) in the treatment of advanced human cancer. Clin Cancer Res 2013;19:1021–1034. [PubMed: 23460533]
6. Brahmer JR, Tykodi SS, Chow LQ, et al. Safety and activity of anti-PD-L1 antibody in patients with advanced cancer. The New England journal of medicine 2012;366:2455–2465. [PubMed: 22658128]
7. Topalian SL, Hodi FS, Brahmer JR, et al. Safety, activity, and immune correlates of anti-PD-1 antibody in cancer. The New England journal of medicine 2012;366:2443–2454. [PubMed: 22658127]
8. Cristescu R, Mogg R, Ayers M, et al. Pan-tumor genomic biomarkers for PD-1 checkpoint blockade–based immunotherapy. Science 2018;362:eaar3593. [PubMed: 30309915]
9. Shien K, Papadimitrakopoulou VA, Wistuba, II. Predictive biomarkers of response to PD-1/PD-L1 immune checkpoint inhibitors in non-small cell lung cancer. Lung Cancer 2016;99:79–87. [PubMed: 27565919]
10. Hodi FS, O'Day SJ, McDermott DF, et al. Improved survival with Ipilimumab in patients with metastatic melanoma. The New England journal of medicine 2010;363.
11. Wolchok JD, Kluger H, Callahan MK, et al. Nivolumab plus Ipilimumab in Advanced Melanoma. The New England journal of medicine 2013;369.
12. Daud AI, Wolchok JD, Robert C, et al. Programmed death-ligand 1 expression and response to the anti-programmed death 1 antibody Pembrolizumab in melanoma. J Clin Oncol 2016;34.
13. Hamid O, Robert C, Daud A, et al. Safety and tumor responses with Lambrolizumab (anti–PD-1) in melanoma. The New England journal of medicine 2013;369.
14. Wang J, Chmielowski B, Pellissier J, et al. Cost-effectiveness of pembrozilumab versus ipilimumab in ipilimumab-naive patients with advanced melanoma in the United States. J Manag Care Spec Pharm 2017;23.
15. Morrison C, Pabla S, Conroy JM, et al. Predicting response to checkpoint inhibitors in melanoma beyond PD-L1 and mutational burden. Journal for ImmunoTherapy of Cancer 2018;6:32. [PubMed: 29743104]
16. Nishino M, Ramaiya NH, Hatabu H, et al. Monitoring immune-checkpoint blockade: response evaluation and biomarker development. Nat Rev Clin Oncol 2017;14.
17. Ayers M, Lunceford J, Nebozhyn M, et al. IFN-γ–related mRNA profile predicts clinical response to PD-1 blockade. The Journal of Clinical Investigation 2017;127:2930–2940. [PubMed: 28650338]
18. Carvajal-Hausdorf DE, Schalper KA, Neumeister VM, et al. Quantitative measurement of cancer tissue biomarkers in the lab and in the clinic. Laboratory Investigation 2014;95:385. [PubMed: 25502176]

19. Schalper KA, Brown J, Carvajal-Hausdorf D, et al. Objective Measurement and Clinical Significance of TILs in Non–Small Cell Lung Cancer. JNCI: Journal of the National Cancer Institute 2015;107:dju435–dju435. [PubMed: 25650315]
20. Camp RL, Charette LA, Rimm DL. Validation of tissue microarray technology in breast carcinoma. Lab Invest 2000;80:1943–1949. [PubMed: 11140706]
21. Anagnostou VK, Syrigos KN, Bepler G, et al. Thyroid transcription factor 1 is an independent prognostic factor for patients with stage I lung adenocarcinoma. J Clin Oncol 2009;27:271–278. [PubMed: 19064983]
22. Wong PF, Wei W, Smithy JW, et al. Multiplex Quantitative Analysis of Tumor-Infiltrating Lymphocytes and Immunotherapy Outcome in Metastatic Melanoma. Clinical Cancer Research 2019.
23. Camp RL, Chung GG, Rimm DL. Automated subcellular localization and quantification of protein expression in tissue microarrays. Nat Med 2002;8:1323–1327. [PubMed: 12389040]
24. Toki MI, Mani N, Smithy JW, et al. Immune Marker Profiling and Programmed Death Ligand 1 Expression Across NSCLC Mutations. J Thorac Oncol 2018;13:1884–1896. [PubMed: 30267840]
25. Gettinger SN, Choi J, Mani N, et al. A dormant TIL phenotype defines non-small cell lung carcinomas sensitive to immune checkpoint blockers. Nat Commun 2018;9:3196. [PubMed: 30097571]
26. Toki MI, Cecchi F, Hembrough T, et al. Proof of the quantitative potential of immunofluorescence by mass spectrometry. Lab Invest 2017;97:329–334. [PubMed: 28092364]
27. Schalper KA, Brown J, Carvajal-Hausdorf D, et al. Objective Measurement and Clinical Significance of TILs in Non–Small Cell Lung Cancer. J Natl Cancer Inst 2015;107.
28. Ma J, Liu L, Che G, et al. The M1 form of tumor-associated macrophages in non-small cell lung cancer is positively associated with survival time. BMC Cancer 2010;10:112. [PubMed: 20338029]
29. Barbieri G, Rimini E, Costa MA. Effects of human leukocyte antigen (HLA)-DR engagement on melanoma cells. Int J Oncol 2011;38:1589–1595. [PubMed: 21455572]
30. Colloby PS, West KP, Fletcher A. Is Poor Prognosis Really Related to Hla-Dr Expression by Malignant-Melanoma Cells. Histopathology 1992;20:411–416. [PubMed: 1587490]
31. Lee N, Zakka LR, Mihm MC, Jr., et al. Tumour-infiltrating lymphocytes in melanoma prognosis and cancer immunotherapy. Pathology 2016;48:177–187. [PubMed: 27020390]
32. Blank CU, Rozeman EA, Fanchi LF, et al. Neoadjuvant versus adjuvant ipilimumab plus nivolumab in macroscopic stage III melanoma. Nature Medicine 2018;24:1655–1661.
33. Amaria RN, Reddy SM, Tawbi HA, et al. Neoadjuvant immune checkpoint blockade in high-risk resectable melanoma. Nature Medicine 2018;24:1649–1654.
34. Tumeh PC, Harview CL, Yearley JH, et al. PD-1 blockade induces responses by inhibiting adaptive immune resistance. Nature 2014;515:568–571. [PubMed: 25428505]
35. Chen PL, Roh W, Reuben A, et al. Analysis of Immune Signatures in Longitudinal Tumor Samples Yields Insight into Biomarkers of Response and Mechanisms of Resistance to Immune Checkpoint Blockade. Cancer Discov 2016;6:827–837. [PubMed: 27301722]
36. Peranzoni E, Lemoine J, Vimeux L, et al. Macrophages impede CD8 T cells from reaching tumor cells and limit the efficacy of anti–PD-1 treatment. Proceedings of the National Academy of Sciences 2018.
37. Gartrell RD, Marks DK, Hart TD, et al. Quantitative Analysis of Immune Infiltrates in Primary Melanoma. Cancer Immunology Research 2018;6:481–493. [PubMed: 29467127]
38. Rosenberg JE, Hoffman-Censits J, Powles T, et al. Atezolizumab in patients with locally advanced and metastatic urothelial carcinoma who have progressed following treatment with platinum-based chemotherapy: a single-arm, multicentre, phase 2 trial. The Lancet 2016;387:1909–1920.
39. Emens L, Loi S, Rugo H, et al. IMpassion130: Efficacy in immune biomarker subgroups from the global, randomized, double-blind, placebo-controlled, phase III study of atezolizumab + nab-paclitaxel in patients with treatment-naïve, locally advanced or metastatic triple-negative breast cancer. In: Proceedings from the 2018 San Antonio Breast Cancer Symposium; December 4–8, 2018; San Antonio, Texas Abstract GS1–04 2018.

40. Motzer RJ, Powles T, Atkins MB, et al. IMmotion151: A Randomized Phase III Study of Atezolizumab Plus Bevacizumab vs Sunitinib in Untreated Metastatic Renal Cell Carcinoma (mRCC). Journal of Clinical Oncology 2018;36:578–578.

41. Rittmeyer A, Barlesi F, Waterkamp D, et al. Atezolizumab versus docetaxel in patients with previously treated non-small-cell lung cancer (OAK): a phase 3, open-label, multicentre randomised controlled trial. The Lancet 2017;389:255–265.

42. Schultheis AM, Scheel AH, Ozretic L, et al. PD-L1 expression in small cell neuroendocrine carcinomas. Eur J Cancer 2015;51:421–426. [PubMed: 25582496]

43. Herbst RS, Soria JC, Kowanetz M, et al. Predictive correlates of response to the anti-PD-L1 antibody MPDL3280A in cancer patients. Nature 2014;515:563–567. [PubMed: 25428504]

44. Hartley GP, Chow L, Ammons DT, et al. Programmed Cell Death Ligand 1 (PD-L1) Signaling Regulates Macrophage Proliferation and Activation. Cancer Immunol Res 2018.

45. Lin H, Wei S, Hurt EM, et al. Host expression of PD-L1 determines efficacy of PD-L1 pathway blockade–mediated tumor regression. The Journal of Clinical Investigation 2018;128:805–815. [PubMed: 29337305]

46. Tang H, Liang Y, Anders RA, et al. PD-L1 on host cells is essential for PD-L1 blockade–mediated tumor regression. The Journal of Clinical Investigation 2018;128:580–588. [PubMed: 29337303]

TRANSLATIONAL RELEVANCE

The NanoString Digital Spatial Profiler (DSP) is a novel platform that offers the capacity of high-plex immune marker quantitative measurements within specific regions of interest. In this study, the DSP technology was shown to have high concordance to the AQUA method of quantitative immunofluorescence (QIF) in non-small cell lung cancer, in most markers. The platform was then used to profile pretreatment biopsies from immunotherapy-treated melanomas by measuring 44 immune markers simultaneously in macrophage, leukocyte and tumor compartments, from which 26 predictive markers of response and survival were identified, demonstrating the discovery potential for the platform. Most notably, we found that PD-L1 in macrophages, but not melanocytes, shows association with response to immunotherapy. While further work is needed to validate this observation and to translate assay to usage in a CLIA lab, this biomarker could improve the sensitivity and specificity of the current PD-L1 IHC companion diagnostic test for immunotherapy.

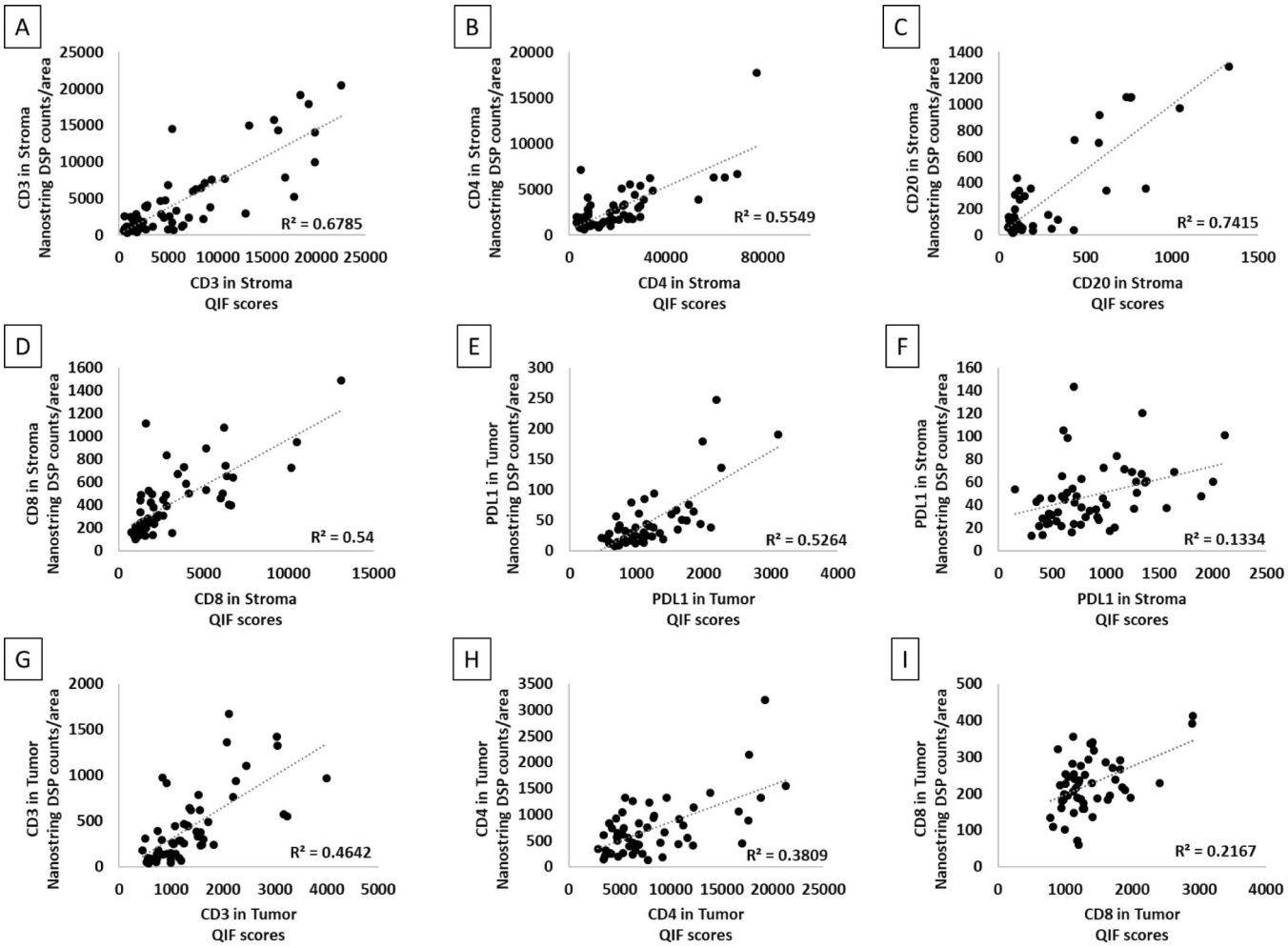

Figure 1: NanoString DSP to QIF comparison in Yale NSCLC cohort A.

Regression of NanoString DSP counts to QIF scores for (A) CD3 in stroma (B) CD4 in stroma (C) CD20 in stroma (D) CD8 in stroma (E) PD-L1 in tumor (F) PD-L1 in stroma (G) CD3 in tumor (H) CD4 in tumor and (I) CD8 in tumor.

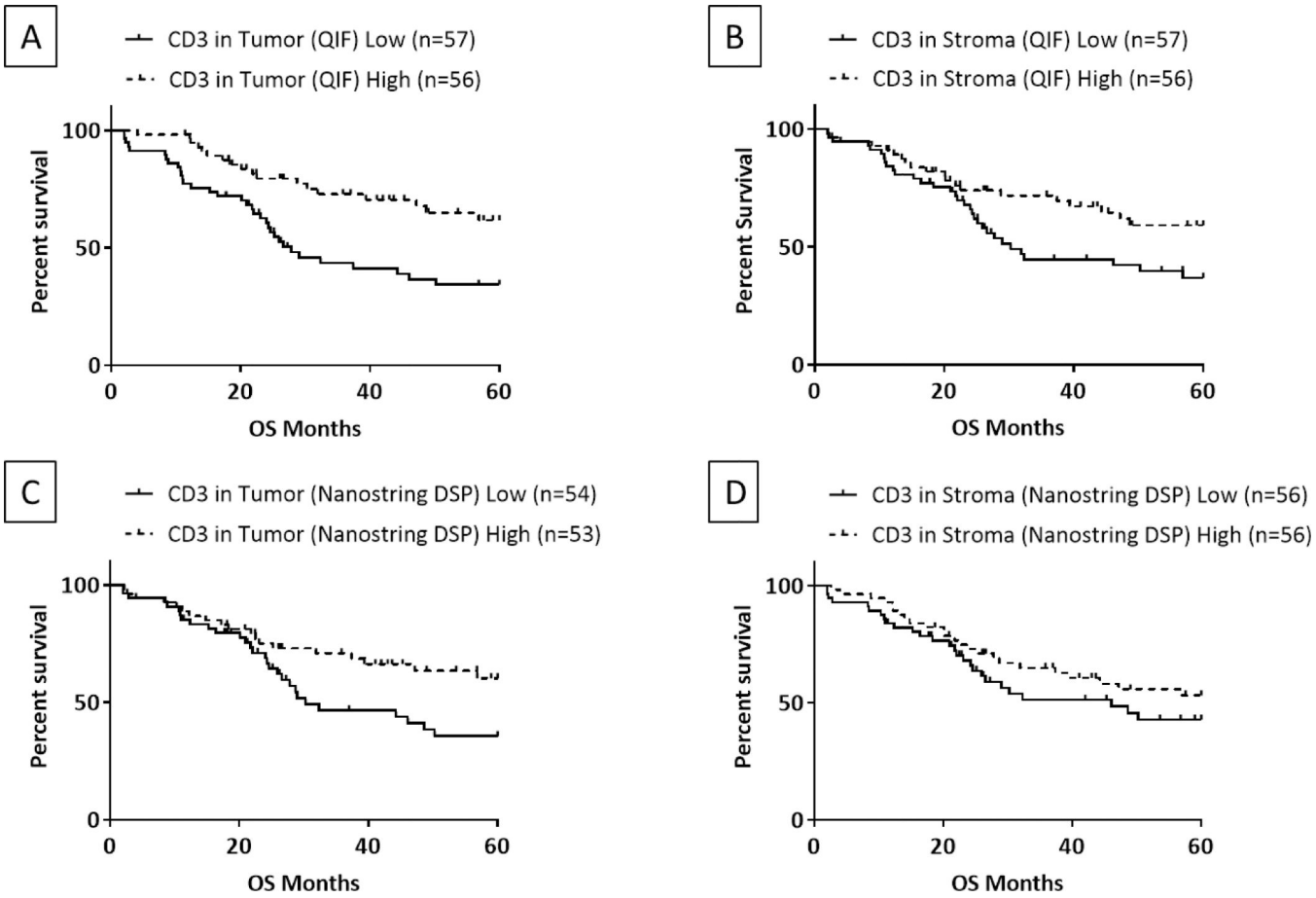

Figure 2: Prognostic value of NanoString DSP and QIF in Yale NSCLC cohort B.

Kaplan Meier 5-year survival curves of NSCLC patients in Yale cohort B, stratified by median tumor and stroma CD3 expression measured by QIF and NanoString DSP. (A) CD3 in tumor by QIF, p=0.0019 HR:0.41, 95% CI: 0.24–0.72 (B) CD3 in stroma by QIF, p=0.036 HR: 0.55, 95% CI: 0.32–0.96 (C) CD3 in tumor by NanoString DSP, p=0.034 HR: 0.54, 95% CI: 0.30–0.95 (D) CD3 in stroma by NanoString DSP, p=0.26 HR: 0.73 95% CI: 0.42–1.27. Survival analysis by log-rank (Mantel-Cox) test.

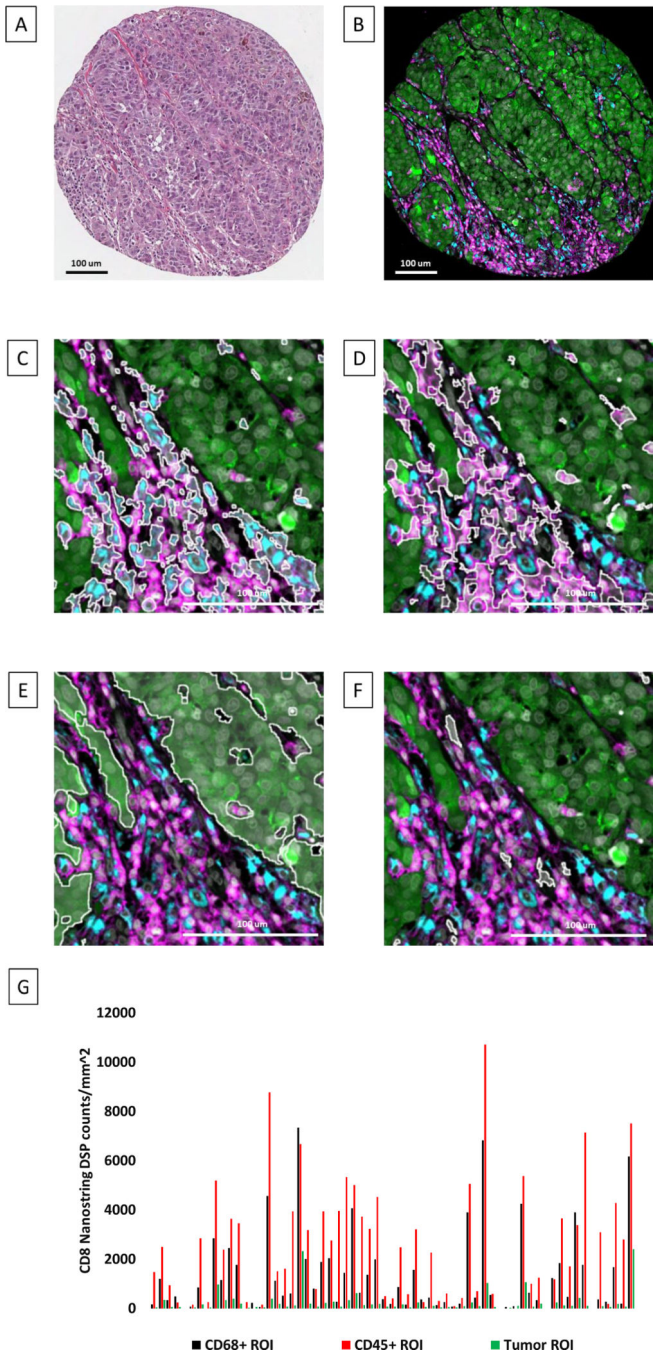

Figure 3: Representative images of NanoString DSP compartment selection in melanoma cohort C.

(A) H&E image of a representative TMA spot (B) Low resolution immunofluorescence image of the markers that define the selected compartments. Melanocytes are in green, CD68+ is in blue and CD45+ is in purple. Selection of (C) CD68+ compartment, (D) CD45+ compartment, (E) tumor compartment and (F) remaining DNA+ compartment.

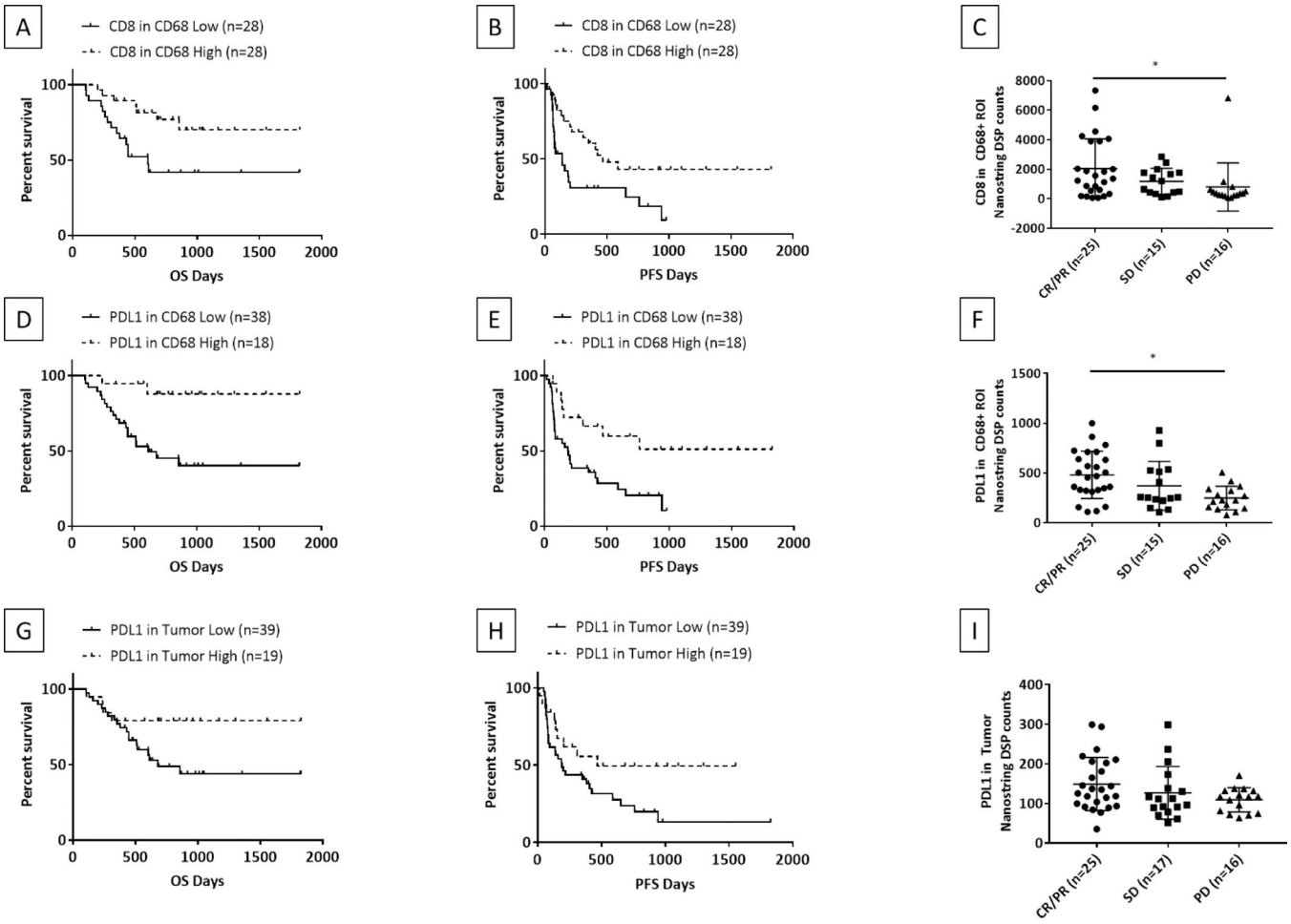

Figure 4: Candidate predictive markers in immunotherapy treated melanoma cohort C by NanoString DSP.

Kaplan Meier 5-year survival and progression free survival curves of immunotherapy treated melanoma patients in Yale cohort C. (A) OS by CD8 counts in CD68+ compartment, p=0.0119 (B) PFS by CD8 counts in CD68 compartment, p=0.0082 (C) Response to ICIs by CD8 counts in CD68+ compartment, p=0.014 (D) OS by PD-L1 in CD68+ compartment, p=0.0032 (E) PFS by PD-L1 in CD68+ compartment, p=0.0072 (F) Response to ICIs by PD-L1 in CD68+ compartment, p=0.011 (G) OS by PD-L1 in tumor compartment, p=0.072 (E) PFS by PD-L1 in tumor compartment, p=0.054 (F) Response to ICIs by PD-L1 in tumor compartment. Survival analysis by log-rank (Mantel-Cox) test. Two-tailed Mann-Whitney U test, bars represent means with standard deviation. *Denotes statistical significance p<0.05.

Table 1:

Summary of all candidate predictive markers for PFS in tumor, CD68+ and CD45+ compartment, log-rank (Mantel-Cox) test.

Predictive markers for PFS														
Tumor ROI	**Cutpoint**	**Hazard Ratio**	**95% CI**	**p value**	**CD68+ ROI**	**Cutpoint**	**Hazard Ratio**	**95% CI**	**p value**	**CD45+ ROI**	**Cutpoint**	**Hazard Ratio**	**95% CI**	**p value**
IDO1	Low (1st and 2nd tertile) vs High (3rd tertile)	0.3205	0.1705 to 0.6026	0.0021	**PDL1**	Low (1st and 2nd tertile) vs High (3rd tertile)	0.3641	0.1899 to 0.6979	0.0072	**B2M**	Median	0.3869	0.1998 to 0.7494	0.0033
CD3	Median	0.4409	0.2331 to 0.8338	0.0099	**CD8**	Median	0.4283	0.2209 to 0.8302	0.0082					
CD8	Median	0.4532	0.2385 to 0.8614	0.0119	**B2M**	Median	0.469	0.2434 to 0.9036	0.0195					
CD11c	Median	0.4669	0.2476 to 0.8804	0.0157	**TIM3**	Median	0.4687	0.2447 to 0.8977	0.0209					
HLADR	Median	0.4998	0.2645 to 0.9443	0.0281										
TIM3	Median	0.5298	0.2822 to 0.9946	0.0482										

Table 2:

Summary of all candidate predictive markers for OS in tumor, CD68 and CD45 compartment, log-rank (Mantel-Cox) test.

Predictive markers for OS														
Tumor ROI	**Cutpoint**	**Hazard Ratio**	**95% CI**	**p value**	**CD68+ ROI**	**Cutpoint**	**Hazard Ratio**	**95% CI**	**p value**	**CD45+ ROI**	**Cutpoint**	**Hazard Ratio**	**95% CI**	**p value**
CD20	Median	0.2581	0.1128 to 0.5904	0.0019	**PDL1**	Low (1st and 2nd tertile) vs High (3rd tertile)	0.153	0.0651 to 0.3598	0.0032	**MSH2**	Low (1st and 2nd tertile) vs High (3rd tertile)	3.277	1.222 to 8.783	0.0035
HLADR	Median	0.2762	0.1212 to 0.6294	0.0035	**CD8**	Median	0.3377	0.1448 to 0.7876	0.0119	**B2M**	Median	0.28	0.11 to 0.67	0.0049
CD8	Median	0.3321	0.1455 to 0.7578	0.01	**B2M**	Median	0.34	0.14 to 0.80	0.0138	**PMS2**	Median	2.763	1.162 to 6.574	0.0211
IDO1	Low (1st and 2nd tertile) vs High (3rd tertile)	0.2392	0.1033 to 0.554	0.0117	**CD3**	Median	0.373	0.1609 to 0.8648	0.0243					
B2M	Median	0.42	0.18 to 0.96	0.0429	**CD4**	Median	0.3741	0.1613 to 0.8672	0.0244					
					PMS2	Median	2.466	1.067 to 5.699	0.0405					
					MYC	Median	2.466	1.067 to 5.7	0.0407					